Iraqi J. Laser, issue 1, vol., 21, pp. 44-50 (2022)

IRAQI JOURNAL OF LASER

Towards C+L Band Three-Mode (De)Multiplexer Using Subwavelength Grating (SWG) Technology

Zaid Lateef Hussain[1], Raad S. Fyath[2]

1University of Baghdad, Institute of Laser for Postgraduate Studies, Baghdad, Iraq
2Al-Nahrain University, College of Engineering, Department of Computer Engineering, Baghdad, Iraq

(Received 05/02/2022; accepted 30/03/2022)

Abstract: Recently, there is increasing interest in using mode-division multipelexing (MDM) technique to enhace data rate transmission over multimode fibers. In this technique, each fiber mode is treated as a separate optical carrier to transfer its own data. This paper presents a broadband, compact, and low loss three-mode (de)multiplexer designed for C+L band using subwavelength grating (SWG) technology and built-in silicon-on-insulator SOI platform. SWG offers refractive index engineering for wider operating bandwidth and compact devices compared to conventional ones. The designed (de)multiplex deals with three modes (TE0, TE1, and TE2) and has a loss > -1 dB and crosstalk < −15 dB, and its operation cover 160 nm (1490 to 1650) nm wavelength span. The overall size of the designed device is 80 × 4 μm^2.

1. Introduction

Demultiplexers are the key elements in mode division multiplexing (MDM) technology and bandwidth expansion [1,2]. Several (de)multiplexing schemes such as Y-junction, micro-ring resonators (MRR), multimode interference (MMI), directional couplers (DC), and coupled waveguides have been reported [3-7]. The MMI coupler has the most interest in multiplexer's design since it offers good performance over a wide bandwidth [8]. Generally, these devices are designed to operate in the C-band range. In MDM, it is preferred to operate with a maximum number of modes and wide operating bandwidth [9]. Expanding the operating bandwidth beyond the C-band is an effective solution to handle capacity issues in the existing optical infrastructure with no need to add new hardware resources [10]. Thus, extending the operating bandwidth towards L-band will allow the use of current technologies to be used over the C+L band [11]. The reason behind considering L-band is due to attenuation losses for C and L bands are approximately the same, also the erbium-doped fiber amplifier can be tuned easily to operate for the new C+L band [12]. Recently, researches have been reported for demultiplexer operating in C+L bands utilizing Y-junctions, directional couplers (DC), and air-core ring fiber [13-17]. Recalling the advantages of the MMI coupler, yet, it is still restricted by the refractive index of the silicon in terms of limited bandwidth and large size and therefore subwavelength grating (SWG) technology has been introduced for refractive index engineering [18]. SWG waveguides are built from two materials arranged periodically as strips in dimensions less than the wavelength of the propagating light. This results in suppression of dispersion effect and an

equivalent homogenous medium with optical properties that combine those of the constructing materials [19]. Applying this technology produces compact, wide-band, and low-loss devices [20].

In this paper, a dual-bandwidth, low loss, compact, and fabrication tolerant three-mode demultiplexer is designed utilizing subwavelength grating (SWG) technology. The device consists of an MMI coupler, a phase shifter, and a splitter to (de)multiplex the three input modes TE0, TE1, and TE2 into a uniform fundamental TE0 mode at the output ports. The results show that the designed device has a loss > -1 dB and crosstalk < −15 dB, 160 nm wavelength span (1490 to 1650) nm covering C+L bands, and 80 × 4 μm^2 overall footprint. The simulation is carried out via Rsoft photonics CAD version 2020.03.

2. Design Dimensioning and Analysis

According to the 100 GHz, IUT wavelength grid issued for wavelength division multiplexing (WDM), each of the L- and C- bands covers 10 THz bands. The L-band covers 50 channels starting from 186 THz (1161.78 nm) to 190.9 THz (1570.41 nm). The C-band covers 50 channels too, starting from 191 THz (1569.59) nm to 195.9 THz (1530.33 nm). Thus C+L starts from 1530.33-1611.78 nm centered at 1569.59 nm which is the designed wavelength of the proposed device. The scheme of the proposed device is shown in Figure 1.

The device is designed using SWG technology and based on an SOI platform with a rib/ridge waveguide structure. The SWG comprising materials are Si (n_{Si}=3.46) and SiO_2 (n_{SiO2}=1.46) arranged periodically as strips of thickness a_i and duty cycle D.C =Λ_i/a_i, repeated over a period $\Lambda_i \ll \lambda_{light}$. The slab and component heights are 0.2 μm and 0.5 μm, respectively. The device consists of three sections, the 1x3 splitter, $\pi/2$ phase shifter, and 3x3 MMI coupler. It handles three input modes TE0, TE1, and TE2 which are converted into a TE0 mode at the output ports.

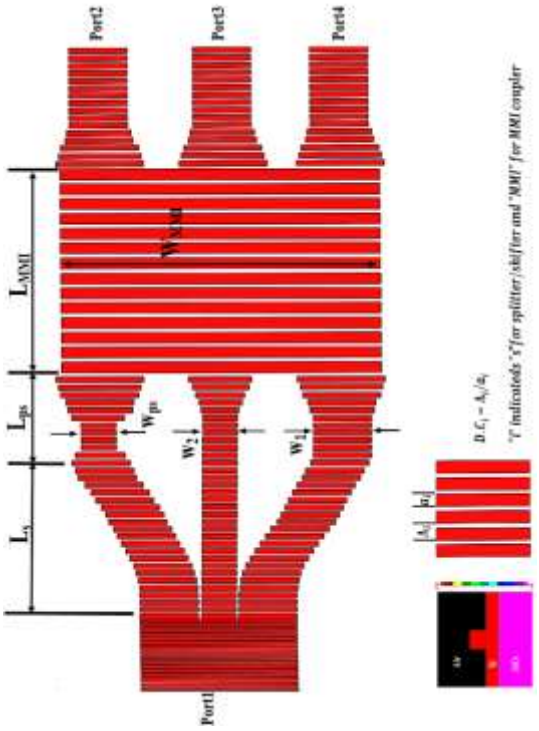

Fig.1: Schematic diagram of the proposed device. The inset is waveguide cross-section and SWG details.

The 1x3 splitter is designed so that TE0 and TE1 modes are split equally to the outer arms (of width w_1), while TE2 is guided through the central arm (of width w_2) only. To satisfy the desired operation, splitter dimensions including pitch length Λ_s (duty cycle (D.C) %), arm length and arms widths L_s, w_1, and w_2 are numerically determined for the optimum performance. Figures 2(a) shows simulation results of the splitter normalized transmission as a function of arm width variation for each one of the input modes. It is obvious that outer arms, for the case of TE0 and TE1, can be guided with maximum transmission and TE2 with minimum transmission when w_1 is set to 0.5 μm (refer to the orange and blue lines). In contrast, for central arm, the maximum transmission of TE2 and minimum transmission of TE0 and TE1 occur when w_2 is 0.27 μm (refer to the red and violate lines) Similarly, the length of the splitter arms is deduced to achieve maximum transmission for each mode. The result is depicted in Figure 2(b) which shows that the optimum value of the length is at L_s= 25 μm. Note that to ensure a smooth transition of the field along the segmented waveguide, the eddect of Λ_s (duty cycle (D.C) %), is simulated and the results are shown in Figure 2(c), and thus Λ_s is set to 0.16 μm yielding D.C. = 70%.

The device transmission characteristics can be obtained as a multiplication of the transmission functions of the three stages compromising the device. Recall that the device consists of three sections, the 1x3 splitter, $\pi/2$ phase shifter, and3x3 MMI coupler. Note that the transfer function of the splitter is wavelength dependent.

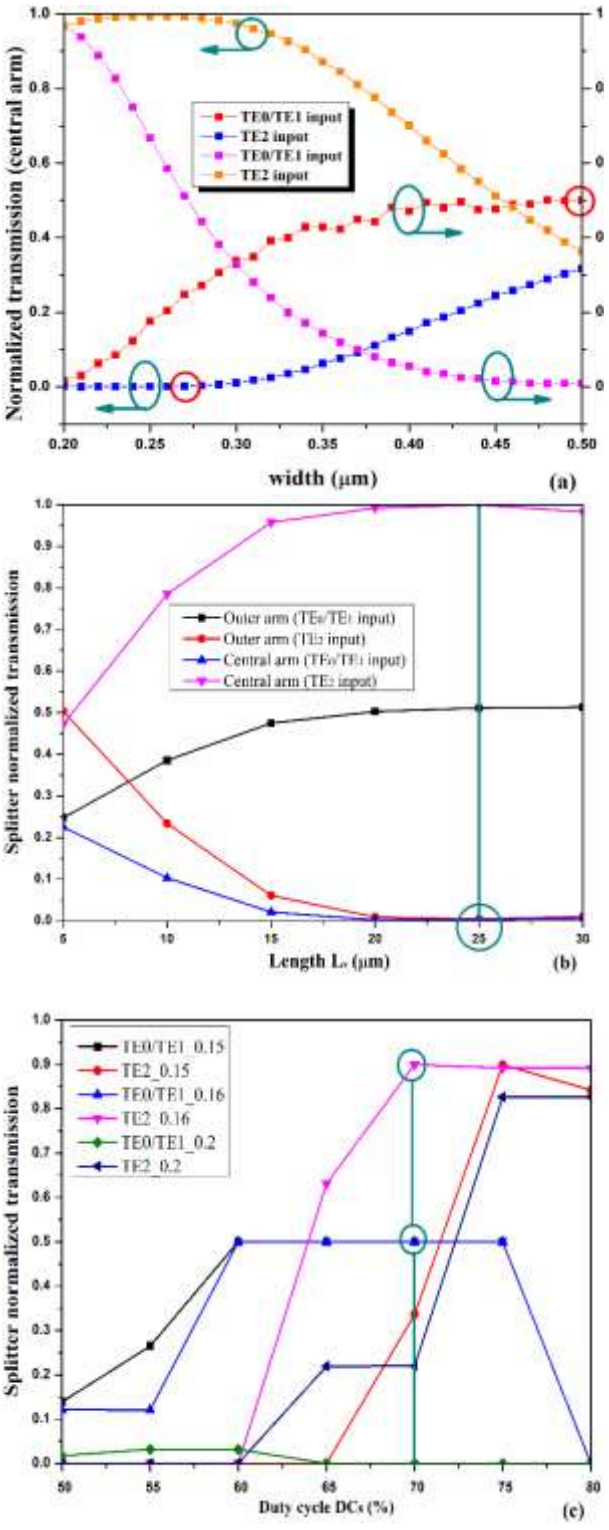

Fig.2: Splitter transmission as a function of arms (a) width (b) length (c) duty cycle.

Next, a $\pi/2$ the phase shifter is designed based on the phase difference between two waveguides of different widths. The shifter is placed at one of the outer arms, thus only TE0 and TE1 cases are affected. The dimensions of the shifter are the length L_{ps} which is set to 3 μm for compactness purposes, and the width w_{ps}. Figure 3 shows the phase difference as a function of width variation w_{ps}. Note that the desired shift can be achieved at any intersection point of the red line curve with the $\pi/2$ margin line. Thus, width $w_{ps} = 0.22, 0.26, 0.31, \text{and } 0.42$ μm can serve the purpose. In this design $w_{ps} = 0.31$ μm is choosen

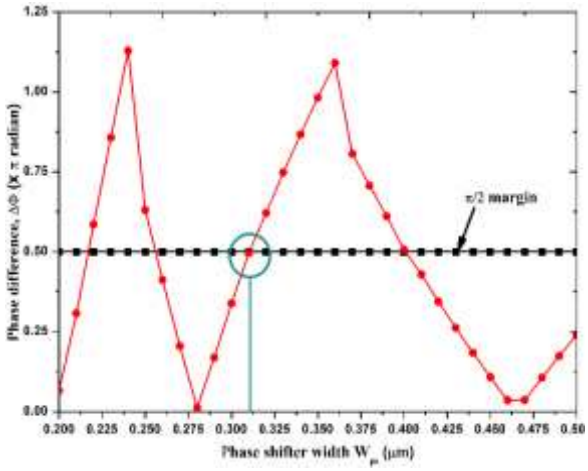

Fig.3: Phase difference as a function of shifter width w_{ps}.

Finally, the 3x3 MMI section is designed. The desired function is to act as a 3-dB splitter for the case of TE0 and TE1 mode (outer input ports), whereas for the TE2 mode case, the field is guided directly from the central input port to the central output port. Thus, it is required to choose MMI length L_{MMI} , width W_{MMI}, pitch length Λ_{MMI} to satisfy these requirements. The MMI length can be expressed in terms of modified beat length L_π formula by the effect of SWG technology as follows [8]

$$L_{MMI} = 1.5L_\pi \quad (1)$$

$$L_\pi = \frac{4n_{eff}W_{MMI}^2}{3\lambda_{light}} \quad (2)$$

where λ_{light} is the wavelength of the light ($\lambda_{light} = 1569.6\,nm$), n_{eff} is the SWG effective refractive index given by [20]

$$n_{eff} = \left[(n_{Si}^2 + n_{SiO_2}^2).\frac{\Lambda}{a}\right]^{1/2} \quad (3)$$

The width W_{MMI} and pitch length (duty cycle %) are set to 4 µm, and 0.2 µm (50%) for compactness purposes, respectively. Numerical simulation for the optimum value of L_{MMI} is carried out around theoretical value calculated from equation (1). Figure 4 presents the response of the MMI coupler as a function of its length. The results show that the suitable L_{MMI} value is 45 µm at which TE0 and TE1 are split equally through the outer ports, whereas the TE2 field is guided directly from the central input to the central output port.

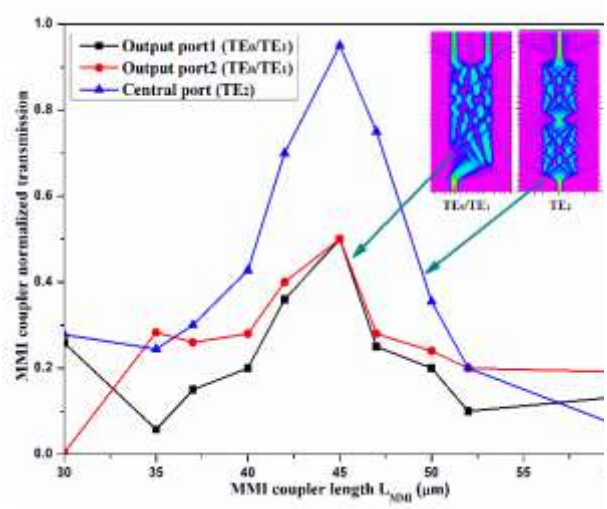

Fig.4: Coupler transmission as a function of the length L_{MMI}.

3. Performance Characteristic and Evaluation

Intensity distribution study along the (de)multiplexer is carried out using Rsoft photonics CAD suit for each case of input modes across the designed device at the operating wavelength λ_{light} = 1569.6 nm. The simulation is repeated for the L+C band corresponding to 1530.3 nm and 1611.8 nm. The results are shown in Figures 5 to 7. The TE0 and TE1 mode split equally through the outer arms and the output for each case is detected from port4 and port2, respectively. For TE2 mode, guided along the central arm of the splitter and the output is detected at port3.

To evaluate the performance of the device, the insertion loss (I.L), and crosstalk (C.T) are calculated for each described case and using the following formula

$$I.L\ (dB) = 10\log(\frac{P_{out}}{P_{in}}) \quad (4)$$

$$C.T\ (dB) = -10\log(\frac{P_{out}}{\sum P_{out\_undesired}}) \quad (5)$$

where P_{in}, P_{out}, $P_{out\_undesired}$ are input power, desired output power from desired port, undesired output power from other ports, respectively. The I.L at the design wavelength > -1 dB and the C.T is better than −17.3 dB.

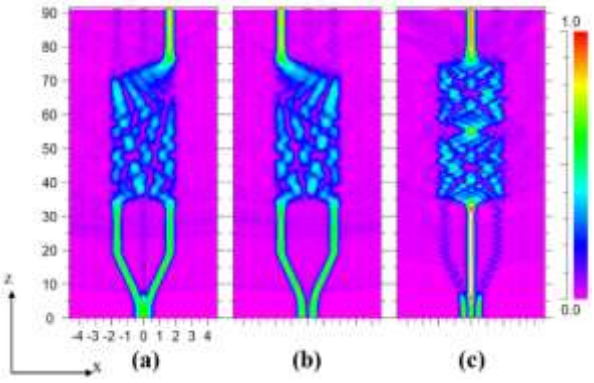

Fig.5: Intensity distribution along the demultiplexer for input mode (a) TE0, (b) TE1, (c) TE2. at 1569.6 nm.

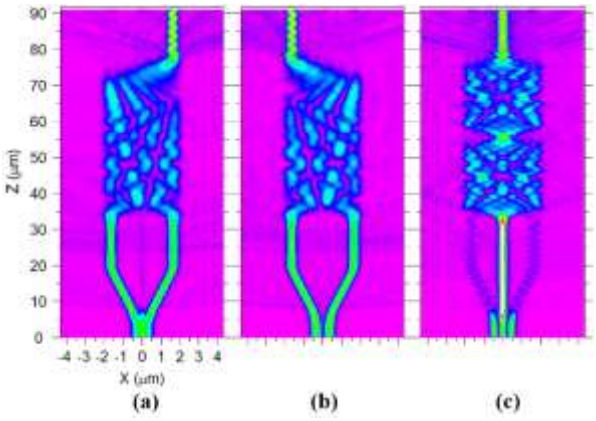

Fig.6: Intensity distribution along the demultiplexer for input mode (a) TE0, (b) TE1, (c) TE2. at 1530.3 nm.

Wavelength (nm)	I.L (dB)			C.T (dB)		
	TE0	TE1	TE2	TE0	TE1	TE2
1530.3	-1.4	-1.7	-1.4	-24	-23	-18
1569.6	-0.8	-0.73	-0.55	-19.3	-22.4	-17.3
1611.8	-1.17	-1.2	-1	-18	-25	-15

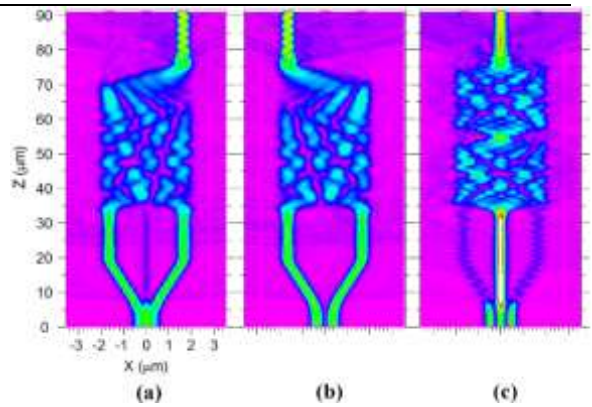

Fig.7: Intensity distribution along the demultiplexer for input mode (a) TE0, (b) TE1, (c) TE2. at 1611.8 nm.

To obtain the operating bandwidth of the designed device, both parameters are plotted over a certain wavelength and the 3 dB threshold from the optimum performance is used. The result is depicted in figure 8. It is clear that the designed device shows good performance of I.L > -3 dB and C.T better than −15 dB over 160 nm operating bandwidth covering (1490 to 1650) nm wavelength span which confirms that the designed device is capable to cover the C+L band of the optical spectrum.

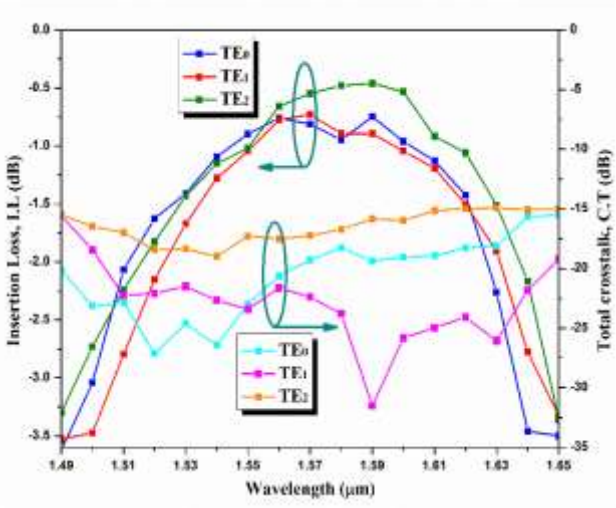

Fig. 8: Demultiplexer response dependency on operating wavelength.

Table 1 lists the insertion loss and crosstalk readings of the proposed device for each of the input mode cases at the wavelengths 1530.3, 1569.6, and 1611.8 nm.

Table (1) Device performance.

4. Fabrication Error Investigation

Errors during the fabrication process that may occur are investigated by checking the response of the proposed device to the deviation of its main parameters from their designed value based on the I.L and C.T measures. Table 2 lists the summary of the allowed fabrication errors measured in nm.

Table (2) Allowed fabrication error summary.

Parameter	Designed (μm)	Fabrication error (nm)	I.L (dB)	C.T (dB)
Λ_{MMI}	0.2	±2	>-2	<-15
w_{ps}	0.21	±15		
w_1, w_2	0.5, 0.3	±17, ±12		
W_{MMI}	4	±20		

5. Conclusions

In conclusion, a dual-band, compact, low loss, the three-mode demultiplexer is designed utilizing SWG technology. With popper parameters selection, such as pitch lengths, duty cycles, widths, and lengths of each part, desired functions can be achieved. The simulation and result show the proposed device has a loss > -1 dB, with 160 nm operating bandwidth extending over (1490 to 1650) nm wavelength span confirming its capability to cover the C+L band of the optical spectrum. Additionally, the device shows a high degree of compactness with an overall area of 80×4 μm^2. The device offers good performance even under fabrication imperfections. Finally, SWG technology served the target to obtain wideband, low loss, and fabrication tolerant devices.

References

[1] H. Xie et al., "An Ultra-Compact 3-dB Power Splitter for Three Modes Based on Pixelated Meta-Structure," IEEE PHOTONICS Technol. Lett., vol. 32, no. 6, pp. 341–344, 2020. doi: 10.1364/OFC-2020-W4C.4.

[2] H. Xie et al., “Highly Compact and Efficient Four-Mode Multiplexer Based on Pixelated Waveguides,” IEEE Photonics Technol. Lett., vol. 32, no. 3, pp. 166–169, 2020. doi: 10.1109/LPT.2020.2964308.

[3] K. T. Ahmmed, H. P. Chan, and B. Li, “Multi-Function Mode Processing Device for Mode Division Multiplexing Optical Networks,” IEEE Photonics Technol. Lett., vol. 33, no. 2, pp. 101–104, 2021. doi: 10.1109/LPT.2020.3041627.

[4] A. Bagheri, F. Nazari, and M. K. Moravvej-Farshi, “Tunable Optical Demultiplexer for Dense Wavelength Division Multiplexing Systems Using Graphene–Silicon Microring Resonators,” J. Electron. Mater., vol. 49, no. 12, pp. 7410–7419, 2020. doi: 10.1007/s11664-020-08522-y.

[5] R. Liu et al., “Integrated Dual-Mode 3-dB Power Splitter Based on Multimode Interference Coupler,” IEEE Photonics Technol. Lett., vol. 32, no. 14, pp. 883–886, 2020. doi: 10.1109/LPT.2020.3002344.

[6] A. Kaushalram et al., “Ultra-broadband fabrication-tolerant mode division (de)multiplexer on thin film Lithium niobate,” Opt. Commun., vol. 475, pp. 126251 (1-8), 2020. doi: 10.1016/j.optcom.2020.126251.

[7] J. P. Nath et al., “Compact Mode Division (de)Multiplexer Based on Collaterally Coupled SOI Waveguides,” IEEE Photonics Technol. Lett., vol. 32, no. 10, pp. 595–598, 2020. doi: 10.1109/LPT.2020.2985959.

[8] A. T. Tran et al., “A new simulation design of three-mode division (de)multiplexer based on a trident coupler and two cascaded 3 × 3 MMI silicon waveguides,” Opt. Quantum Electron., vol. 49, no. 426, pp. 1-15, 2017. doi: 10.1007/s11082-017-1248-4.

[9] W. K. Zhao et al., “Broadband five-mode (de)multiplexer with horizontal tapered directional couplers,” in: Asia Communications and Photonics Conference, 2017, pp. Su3K.7. doi: 10.1364/ACPC.2017.Su3K.7

[10] M. Cantono et al., “Opportunities and Challenges of C+L Transmission Systems,” J. Light. Technol., vol. 38, no. 5, pp. 1050–1060, 2020. doi: 10.1109/JLT.2019.2959272.

[11] T. Ahmed et al., “C + L-band upgrade strategies to sustain traffic growth in optical backbone networks,” J. Opt. Commun. Netw., vol. 13, no. 7, pp. 193–203, 2021. doi.org/10.1364/JOCN.427097.

[12] K. Minoguchi et al., “Beyond 100-Tb/s ultra-wideband transmission in S, C, and L bands over single-mode fiber,” Next-Generation Opt. Commun. Components, Sub-Systems, Syst. IX, vol. 11309, pp. 113090I (1-9), 2020. doi: 10.1117/12.2541990.

[13] W. K. Zhao, K. X. Chen, and J. Y. Wu, “Broadband mode multiplexer formed with non-planar tapered directional couplers,” IEEE Photonics Technol. Lett., vol. 31, no. 2, pp. 169–172, 2019. doi: 10.1109/LPT.2018.2887352.

[14] H. Shu, B. Shen, Q. Deng, M. Jin, X. Wang, and Z. Zhou, “A Design Guideline for Mode (DE) Multiplexer Based on Integrated Tapered Asymmetric Directional Coupler,” IEEE Photonics J., vol. 11, no. 5, pp. 1–12, 2019. doi: 10.1109/JPHOT.2019.2941742.

[15] W. K. Zhao et al., “Reconfigurable Mode (De)multiplexer with Integrated Thermo-Optic Long-Period Grating and Y-junction,” 2018 Conf. Lasers Electro-Optics, CLEO 2018 - Proc., vol. 30, no. 24, pp. 2119–2122, 2018. doi: 10.1364/OL.43.002082.

[16] D. Chen et al., “C + L band polarization rotator-splitter based on a compact S-bend waveguide mode demultiplexer,” Opt. Express, vol. 29, no. 7, pp. 10949, 2021. doi: 10.1364/oe.412992.

[17] Y. Wang et al., “Air-Core Ring Fiber Guiding >400 Radially Fundamental OAM Modes across S + C + L Bands,” IEEE Access, vol. 9, pp. 75617–75625, 2021. doi: 10.1109/ACCESS.2021.3078504.

[18] L. Sun et al., “Subwavelength structured silicon waveguides and photonic devices,” Nanophotonics, vol. 9, no. 6, pp. 1321–1340, 2020. doi: 10.1515/nanoph-2020-0070.

[19] D. Zhu et al., “High-Contrast and Compact Integrated Wavelength Diplexer Based on Subwavelength Grating Anisotropic Metamaterial for 1550/2000 nm,” IEEE Photonics J., vol. 13, no. 2, 2021. doi: 10.1109/JPHOT.2021.3061966.

[20] S. Han, W. Liu, and Y. Shi, “Ultra-Broadband Dual-Polarization Power Splitter Based on Silicon Subwavelength Gratings,” IEEE Photonics Technol. Lett., vol. 33, no. 15, pp. 765–768, 2021. doi: 10.1109/LPT.2021.3095257.

نحو مُضاعِف ارسال ثلاثي النمط بنطاق C + L
و باستخدام تقنية المحزز مادون الطول الموجي

زيد لطيف حسين* , رعد سامي فياض**

*معهد الليزر للدراسات العليا, جامعة بغداد, بغداد, العراق
**جامعة النهرين, كلية الهندسه, قسم هندسة الحاسوب, بغداد, العراق

الخلاصة: يقدم هذا العمل مضاعف إرسال ثلاثي ا لنمط واسع النطاق, مدمج, ومنخفض الخسارة صمم لتغطية نطاق C+L باستخدام تقنية المحزز مادون الطول الموجي (SWG) ومنصة SOI . تقدم تقنية ال SWG هندسة معامل الانكسار لعرض نطاق تشغيل أوسع وأجهزة مدمجة مقارنة بقريناتها التقليدية. يتعامل مضاعف الإرسال المصمم مع ثلاثة انماط TE0 TE1و TE2 وله خسارة > -1 ديسيبل وتداخل < -15 ديسيبل. الجهاز المصمم يغطي تشغيله 160 نانومتر (1490 إلى 1650 نانومتر) من الطول الموجي. الحجم الكلي للجهاز المصمم 80 × 4 ميكرومتر مربع.